The FASEB Journal express article 10.1096/fj.00-0837fje. Published online July 24, 2001.

Cell cycling determines integrin-mediated adhesion in osteoblastic ROS 17/2.8 cells exposed to space-related conditions

Alain Guignandon,* Marie-Hélène Lafage-Proust,* Yves Usson,† Norbert Laroche,* Anne Caillot-Augusseau,* Christian Alexandre,* and Laurence Vico*

*Laboratoire de Biologie et de Biochimie du Tissu Osseux–Equipe Mixte INSERM E9901, Université Jean Monnet, 15 rue Ambroise Paré, F-42023 Saint-Etienne Cedex 2, Saint-Etienne, France; †Laboratoire TIMC UMR 5512, Institut Albert Bonniot, Université Joseph Fourier, Grenoble, Domaine de la Merci, F-38706 La Tronche Cedex, France

Corresponding author: Christian Alexandre, LBBTO–INSERM E9901, 15 rue Ambroise Paré, F-42023 Saint-Etienne Cedex 2, Saint-Etienne, France. E-mail: guignand@univ-st-etienne.fr

ABSTRACT

Six days of microgravity (Bion10 mission) induced dramatic shape changes in ROS 17/2.8 osteoblasts (7). During the Foton 11 and 12 space flights, we studied the kinetics (0–4 days) of ROS 17/2.8 morphology and adhesion, the relationships between adhesion and cell cycle progression after 4 days in space, and osteoblastic growth and activity after 6 days in space. Quantitative analysis of high-resolution adhesion [focal adhesion area imaged by total interference reflection fluorescent microscopy (TIRFM)] and integrin-dependent adhesion (imaged on confocal microscope by vinculin and phosphotyrosine staining) as well as cell cycle phase classification [Ki-67 staining, S-G2, mitotic cells and G1 (postmitotic cells)] were performed using programs validated in parabolic flight and clinostat. We observed disorganization of the cytoskeleton associated with disassembling of vinculin spots and phosphorylated proteins within focal contacts with no major change in TIRFM adhesion after 2 and 4 days of microgravity. Postmitotic cells, alone, accounted for the differences observed in the whole population. They are characterized by immature peripheral contacts with complete loss of central spots and decreased spreading. Osteocalcin, P1CP and alkaline phosphatase, and proliferation were similar in flight cells and 1 g centrifuge and ground controls after 6 days. In conclusion, microgravity substantially affected osteoblastic integrin-mediated cell adhesion. ROS17/2.8 cells responded differently, whether or not they were cycling by reorganizing adhesion plaque topography or morphology. In ROS 17/2.8, this reorganization did not impair osteoblastic phenotype.

Key words: microgravity • weightlessness • adhesion • cell cycle • osteoblasts • confocal microscopy • TIRFM • image analysis

The importance of cell shape and cytoskeletal changes in the control of cell cycle progression by the extracellular matrix has been particularly emphasized in several adherent cell types such as hepatocytes (1), endothelial cells (2), and fibroblasts (3). Cytoskeletal reorganization during cell spreading or rounding is driven by mechanical tension through the actomyosin machinery and transmitted across the cell surface by integrin receptors to the extracellular matrix. In addition, there is a large body of evidence to suggest that integrins play a central role in the cell response when cells are submitted to external mechanical forces (4). The balance between external and internal forces, partly driven by integrin binding and cell spreading, acts at different points during the cell cycle to direct cells to either live or die (5), to proliferate or to exit the cell cycle, and to differentiate(6).

During the Biocosmos 10 mission, we observed that osteoblastic ROS 17/2.8 cells exhibited dramatic shape changes after 4 days of microgravity: Some cells were rounder and piled up, whereas others were retracted and presented long cytoplasmic extensions. A third population remained spread out, with a similar shape to that of ground controls and in-flight 1 g centrifuge control cells (7). Because these cells were clonal, we hypothesized that this heterogeneous response to microgravity exposure in terms of cell shape could be related to cell cycle phases. In addition, we found that cell shape was highly sensitive to gravitational stresses (2 g, 10^{-2} g) such as those exerted by parabolic flights (8). In a subsequent parabolic flight, we began to study the organization of a known target for mechanical signals: the focal adhesion plaque that constitutes one signaling pathway for transmission of outside/inside information by linking the extracellular matrix to the cytoskeleton and triggering signal transduction cascades (9). We developed an approach for quantitation of focal contacts, based on multimodal confocal microscopy and analysis of immunocytochemistry images (10). We chose vinculin as the molecule representative of focal contact, because it is one of the last proteins that colocalize in the integrin cluster only when integrins have bound to the extracellular matrix (11). Vinculin is responsible for the stiffness of the transmembrane integrin linkages to the cytoskeleton (12, 13) and activates protein tyrosine kinases that play a central role in integrin-mediated signaling (14). We thus found significant parabolic flight-induced cell shape changes, including decreased cell area associated with focal contact plaque reorganization (15). This reorganization comprised a reduction of both the number of vinculin-positive focal contacts and physical adhesion of cells to the substratum as assessed by total interference reflection fluorescent microscopy (TIRFM) imaging. Therefore, as a first step, we demonstrated that the adhesion pattern of ROS 17/2.8 cells was sensitive to g variations induced by parabolic flights.

In these cells, we also observed that, at the time of mitosis, they progressively lost stress fibers and peripheral adhesion plaques as well as became rounder and less adherent in order to divide (data not shown). Daughter cells then spread and developed thick and regularly oriented microfilament bundles of stress fibers ending at vinculin-rich areas of focal contact. Our expectation during microgravity exposure is that the critical step for cell adhesion would be on completion of mitosis, when new cells start to spread.

Based on all these results, and those of Papaseit et al. (16) demonstrating that microtubule assembly was found to be dependent on the g vector in vitro, our working hypothesis is that microgravity is able to modify the dynamic organization of cytoskeletal structures. Indeed, they polymerized/depolymerized continuously, requiring low energy, but through amplifications, they

generated high tension forces to the substratum. Thus, in the present study, we focused on cytoskeletal focal adhesion structures with high-resolution image analysis procedures. Before capsule propulsion into orbit and exposure to microgravity, cells were maintained in low metabolic state by means of low serum (Foton 12) or low temperature (Foton 11) to avoid the potential effects of transportation, prelaunch, and launch (17). Several hours after exposure to microgravity, cells were metabolically activated and kinetics of adhesion changes was quantified at different time points during flights.

Due to space constraints and limited sampling, the experimental design was organized as follows. Changes in the pattern of TIRFM-defined focal contact and vinculin-positive adhesion plaques after 12 h and 4 days of microgravity were quantitatively analyzed in ROS 17/2.8 cells. Actin stress fibers and tyrosine-phosphorylated proteins were also visualized at various time points. We then analyzed the relationships between cell cycle and adhesion pattern on day 4 of the space mission to ensure that several cell generations had occurred in space. Finally, we checked that ROS 17/2.8 cells retained similar growth ability in flight and in control groups, as previously found in these cell types (7) and in other osteoblastic cells (18–21). We also showed that ROS 17/2.8 retained their main osteoblastic features (synthesis of alkaline phosphatase, collagen type I, and osteocalcin) after a 6-day microgravity exposure.

Two space missions were required to achieve our objectives. Shorter exposures to microgravity (Foton 12, 2 days; Foton 11, 4 days) were used to study cell adhesion and its related cell cycle dependency. Samples harvested during the Foton 11 mission (day 4 and 6) were devoted to confirming the osteoblastic phenotype.

MATERIALS AND METHODS

Space flights

Both the Foton 11 and Foton 12 space flight experiments were carried out on the Russian Foton unmanned recoverable capsules. Capsules were launched into polar orbits by Soyuz vehicles from the Plesetsk base (650 km north of Moscow). Capsules flew through space for 12 days for Foton 11 and 15 days for Foton 12. They then left microgravity to return to Earth and landed in Kazakhstan, south of Samara. Two different incubator instruments were used in these missions: the European Space Agency Biobox instrument for Foton 11 and the Centre National d'Etudes Spatiales (French Space Agency) Ibis instrument for Foton 12. Both incubators (Biobox and Ibis) provide identical automated culture conditions, absence of CO_2 exchange, possibility to inject products into the medium during the flight, sample fixation, and in-flight centrifuge (C) generating 1 g and acting as a control with in-flight static culture (flight μg, F). Centrifuge and flight cultures experienced the same vibrations mainly due to take-off. The 1 g centrifuge was used as the in-flight unit-gravity reference. Static ground cultures at 1 g (G) were also performed to test the effects of space flight conditions. After capsule landing, the fixed or lysed cell cultures were kept at 4°C during transportation and were directly processed for immunohistochemistry or biochemical measurements on their arrival at the laboratory. We have previously established, in ground experiments, that antigenic sites were not altered by storing fixed samples at 20°C for 10 days. The feasibility of biochemical measurements was previously studied during the Foton 10 mission (7).

Characteristics for Foton 11 mission (Biobox3)

Before launch, material required for our experiment was transported from Saint-Etienne (France) to the ESA laboratory in Noordwijk (The Netherlands), where our experiment was prepared and installed in the Biobox® Instrument. ROS 17/2.8 cells were plated 2 days before launch at 5 10^3 cells/cm^2 on glass coverslips (Nunc, Life Technologies) and were transferred after 24 h to "Plunger box experiment units" (CCM, Leiden, The Netherlands). These units contain a single 2-ml culture chamber with a culture area of 2 cm^2. The culture chamber is connected to six compartments, each containing a soft plastic bag in which medium, fixative, or lysis buffer is stored. These liquids are forced into the culture chamber by releasing a spring-loaded plunger by sequential electrical activation, allowing medium and fixative buffer changes according to the preprogrammed activation timeline.

A total of 11 experimental units were used for flight conditions, 8 of which were integrated into a static rack (cell in space box) and 3 on a 1 g centrifuge in the Biobox incubator. Ground conditions consisted of 8 experimental units integrated into the cell in space box within an identical Biobox. During the 24 h between integration and launch, cells were maintained quiescent by lowering the temperature to 20°C, after which the temperature in the Biobox was increased to 37°C. Medium was changed and collected daily, and cells were lysed on day 4 or 6. The ground control experiment started after a delay of 3 h and exactly followed the same protocol and temperature profile.

Characteristics for Foton 12 mission (IBIS2)

The Ibis® instrument is divided into three distinct zones: a cold chamber (4°C), where cells cultured in cassettes are stored; a transfer zone between the cold and hot chambers; and a hot chamber (37°C), where cells are cultured under microgravity conditions. The instrument also comprised a continually rotating centrifuge that subjects control samples to acceleration simulating Earth's gravitational forces (1 g control).

The experiment was prepared at the Plessetsk launch base (Russia). Osteoblastic ROS 17/2.8 cells were plated as described for the Foton 11 mission. The culture chamber consisted of a single bag (2 ml) containing the glass coverslip (2 cm^2) and two compartments, one containing serum (cell cycling induction) and the other containing fixative (4% paraformaldehyde solution). These liquids can be delivered into the culture compartment according to the preprogrammed activation timeline.

Cell culture

The cells used in this study were rat osteosarcoma cells (ROS 17/2.8). They were chosen because they possess a well-defined, mature osteoblastic phenotype and because their focal contacts were large and well delimited, allowing image analysis (see below). Products were provided by Sigma Chemical (St. Quentin Fallavier, France). The culture medium was Dulbucco's modified Eagle's medium supplemented with 10% fetal calf serum, 2 mM L-glutamine, and 1% penicillin–streptomycin solution. Because no gas exchange occurs in our culture device, medium was

buffered with 3.7 mg/l of $NaHCO_3$ and 20 mM HEPES. Under these conditions, cell growth and alkaline phosphatase activity are similar to those under normal O_2/CO_2 culture conditions (1).

Fluorescence staining

Cells were washed in phosphate-buffered saline (PBS) and permeabilized with 0.1% Triton X100 for 5 min. Nonspecific binding was blocked by incubation at 37°C in PBS/1% bovine serum albumin. Antivinculin primary antibody (h-vin1 diluted to 1/100) [or anti-phosphotyrosine PY20 (Tebu, France)] and conjugated FITC (1/64) were purchased from Sigma. Ki-67 primary antibody was purchased from Tebu and conjugated TRITC was purchased from Sigma. Antibody incubations were performed at 37°C for 45 min. Cells were washed extensively in PBS between antibody incubations and were mounted in PBS/glycerol (20%) before confocal scanning laser examination. F-actin was stained using BODIPY-FL phallacidin (B-607 Molecular Probes, Leiden, The Netherlands). In brief, cells were rinsed with PBS (pH 7.4) and incubated for 20 min at room temperature before confocal scanning examination.

Image analysis

Adhesion

Cell shape was analyzed with a semiautomatic image analyzer (SAMBA-Alcatel®) on 100 cells per condition. The confocal scanning laser microscope was used to visualize vinculin or phosphotyrosine immunostaining (called spots). TIRFM was used to visualize close contacts between cells and substratum (called plaques). Quantification was based both on thresholding of vinculin or phosphotyrosine adhesion spots and on mathematical processing of TIRFM images. Regions of interest (cell contours) were defined manually. Image processing allowed the calculation of 24 parameters describing morphologic parameters of adhesion plaques and spots, topographic parameters, and interactions between fluorescent spots and TIRFM images by extracting data on overlap areas of spots and plaques (14). The 12 most important parameters among these 24 are described in Figure 1.

Cell cycle phases

Ki-67 proliferation-associated antigen was revealed by immunostaining simultaneously with vinculin staining. This combination allowed the cell cycle phase to be correlated with adhesion pattern cell by cell. The image analysis program used for specific adhesion quantification was also applied for quantification of nuclear parameters (Fig. 1). The number of cells quantified was determined to obtain a minimum of 40 cells per cell cycle phase. The Ki-67 antigen content increases during the cell cycle progression from G1 to M phases. Cell cycle phases could be discriminated according to the particular Ki-67 spot topography (22, 23). Our image analysis software therefore calculated nucleus area, Ki-67 relative area (Ki-67 area divided by nucleus area), and topographic parameters describing the location of Ki-67 staining according to the distance from nucleus edge. The following phases were studied. Mitotic cells were defined as cells with the smallest nucleus area (NA<150 μm^2), associated with the highest Ki-67 relative area (RS>30% of the nucleus area). Postmitotic (Post-M) cells, corresponding to the G0/G1 phases of the cell cycle, presented the lowest Ki-67 relative area (RS<10%) and central punctate

staining, characterized by an elevated average distance of Ki-67 spots from nucleus edge (DS>66%). Furthermore, premitotic (pre-M) cells, corresponding to the S/G2 phases of the cell cycle, were selected by default and represented all other cells. Unstained Ki-67 cells (5% of the cell population) were obviously not taken into account in this part of our study.

Cell counting

Cell proliferation was assessed by direct counting of Ki-67 stained cells per images (day 0, 1, 2, and 4 of the FOTON 12 mission). We also measured the protein content of lysed cells with Bradford method (day 0, 4, and 6 of the FOTON 11 mission)

Biochemical measurements

Alkaline phosphatase activity was measured using *p*-nitrophenylphosphate as substrate according to the Lowry method (24). Cells were washed in PBS and disrupted in TRIS HCl buffer containing 0.1% Triton X100 during the flight. The enzymatic activity was assessed for 30 min at 37°C. Absorbance was read at 405 nm. Results are expressed in nM/l/min/mg of protein. C-terminal type I procollagen propeptide (P1CP, μg/mg protein) was determined by an enzyme-linked immunoassay (Orion Diagnostica, Espoo, Finland). Osteocalcin was assayed in duplicate by a radioimmunoassay (RIA) using an anti-osteocalcin polyclonal immune serum, depending on the epitopes recognized by antibodies to the intact molecule and the fragments (OSTEO-KPR) (CIS bio International). P1CP and Osteocalcin were determined in recovered media collected in individual bags after each medium renewal.

Timeline of the experiment

The timeline of the experiments is described in Figure 2. In the Foton 12 mission, cells were maintained dormant by low serum (1%) culture conditions and proliferation was initiated after 12 h of flight by serum induction (10%). Cells fixed on day 1 were devoted to vinculin staining, and cells fixed on day 2 were devoted to vinculin and phosphotyrosine stainings. In the Foton 11 mission, cell cultures switched from 20 to 37°C after 3 h of flight and they were fixed on day 4 for vinculin, Ki-67, and actin stainings. Biochemical markers were measured in cell lysates after 6 days of microgravity and in medium collected during medium changes on days 0, 2, 4, and 6.

Statistical analysis

For image analysis, 100–150 cells were analyzed at each time point and for each condition. Multivariate analysis tools were used to discriminate groups and to assess the significance of measurements (or variables). Initially, all data were pooled and the correlation matrix was calculated. Factorial discriminant analysis is a multivariate statistical analysis designed to emphasize the difference between experimental groups, based on measurements of several parameters (25). Comparisons between F, C, and G groups were based on the most discriminant parameters, using the Friedman test. When the Friedman test was significant, the Mann-Whitney test was used to compared C versus G and either F versus C or F versus G (with an α-level $\approx$ [nominal α] $\times$ [number of comparisons made]. Nonparametric tests were also used to compare biochemical parameters between groups.

RESULTS

Proliferation and differentiation indices

Both protein content and direct counting of cells were identical between controls, centrifuge, and flight cells all over the culture periods in both missions (Table 1). Osteoblastic differentiation parameters, that is, alkaline phosphatase activity, P1CP, and osteocalcin production were similar between the three conditions, their level being rather constant during the different time points of the mission (Table 1). No normalization has been attempted for P1CP and osteocalcin because conditions between media collections and cell fixation or protein content evaluation did not correspond for each time point.

Morphologic and topographic parameters

Qualitative examination of cell morphology, cytoskeleton and adhesion pattern

Observation of cells by phase contrast microscopy (immediately after retrieval of culture units) did not reveal any differences in cell morphology between ground controls, centrifuge controls, and flight groups after a 1- or 2-day period. However, after 4 days of microgravity, the flight group exhibited morphologic differences, characterized by rounder and smaller cells, compared with centrifuge and ground controls (Fig. 3A, B). In addition, F-actin staining showed a cortical pattern of actin network and disappearance of large bundles of stress fibers in microgravity conditions (Fig. 3C, D). Lastly, confocal images showed more diffuse vinculin spots in flight cells (Fig. 3E, F). No obvious differences were visible between ground and centrifuge controls in the apparent diffusion of vinculin out of the focal contact plane noted in flight groups. Ki-67 staining was seen in each group (Fig. 3G, H) and showed that ROS cells were dividing.

Quantitative cell adhesion parameters

Discriminant analysis of cell adhesion parameters Table 2A summarizes the stepwise factorial discriminant analysis, indicating the discriminant power of each parameter in all the groups at every time point. Restricted factorial discriminant analysis to the ground groups (G0, G1, G2, and G4) on the one hand or to the centrifuge groups (C0, C1, C2, and C4) on the other hand showed that MS (mean area of vinculin spots) was the most discriminant parameter factorial discriminant analysis applied to the flight groups alone (F0, F1, F2, and F4) and showed that RS (relative area of vinculin spots) was the most one. Table 2B shows the a posteriori classification of cells using discriminant parameters to re-affect cells in their defined groups. This classification indicated cell percentage correctly affected in the proper group. The best result was found for cells cultivated 4 days in flight, centrifuge, or ground conditions and to a lesser extent for 2-day cultures as compared with earlier cultures (day 0 and 1). This classification showed that effects of microgravity conditions were modulated by time of exposure. Cultures without serum (T0, G0, C0, and F0) were indistinguishable from each other. This result indicated that cells maintained in a slow metabolic state are not responsive to gravitational alterations.

Differences between groups As early as 24 h of flight, mean area of vinculin spots (MS) was significantly decreased compared with centrifuge or ground controls (Fig. 4A). After 2 days in

space, similar results were seen for vinculin relative area (RS), overlap of vinculin spots with TIRFM focal contact plaques (OSP), and average distance of vinculin spots from the cell edge (DS) that constituted the following discriminant parameters by decreasing order (Fig. 4B–D). The decrease in OSP, which followed the kinetics of RS (i.e., vinculin spots), reflected an uncoupling between vinculin spots and plaques occupancy in microgravity. Furthermore, after 2 days of flight, PY-20 staining indicated that phosphotyrosine-positive spot number (data not shown) and phosphotyrosine-related area were also significantly decreased (-50%) (Fig. 5) compared with both C and G groups. The ratio of phosphotyrosine/vinculin spots was dramatically reduced in microgravity (1.52 versus 2 on ground), suggesting that vinculin left the focal contacts and that transduction activity of this signaling molecule was reduced. After 4 days of flight (Fig. 4), all morphologic and topographic adhesion parameters remained low. Distribution of vinculin spots was now located at the cell periphery as shown by reduced average distance from cell edge to spots (DS -25%). The longer the flight, the greater the differences.

Adhesion cell cycle dependency

Discrimination of adhesion according to cell cycle phases was done after 4 days in microgravity to ensure that we analyzed the second or third generation of ROS 17/2.8 grown is space. To test whether microgravity was able to modify adhesion according to cell cycle phase, factorial discriminant analysis was applied to premitotic, mitotic, and postmitotic cells. Table 3A shows the most discriminant parameters in the cell cycle study. The matrix of classification (Table 3B) indicated that Pre-M and M cells were poorly correctly re-affected (from 12–46%) compared with the better classification of Post-M groups (62–64%). It indicated that microgravity conditions are more discriminant in Post-M cells than in Pre-M or M cells. The variation of discriminant parameters according to cell cycle phases is shown in Table 4. In mitotic cells, no difference between C, G, and F was observed for any of the parameters. In G and C postmitotic cells, the events that followed mitosis were characterized by the formation of new focal contacts (N +100%) associated with a very marked increase in cell area (CA +300%), whereas the topography of focal contacts (DS) was reorganized to remain distributed as in the other phases, suggesting a high turnover of contact formation. Post-M cells of the flight group exhibited a significantly lower vinculin spot number (N -60%); the remaining vinculin spots were smaller (MS -50%) and more peripheral (lower DS). More detailed topographic analysis revealed that flight cells maintained their central (under the nucleus) and peripheral spots, but no spots were observed between these two sites (Fig. 6). In addition to this alteration of adhesion, cell spreading was also reduced [CA × 2 (CA × 3 in controls)]. The main difference in terms of cell cycle progression in the flight group compared with control groups was the reduced amplitude of cell area changes from one phase to another. As for G1 to G2 progression, we found that only mean contact area (MS) normalized during flight, whereas the other parameters remained lower than in control groups. These results indicated that mitotic cells were not affected by microgravity, whereas postmitotic cells appeared to be the most sensitive to microgravity.
Typical examples of changes of adhesion pattern according to cell cycle phase in centrifuge and flight samples are presented in Figure 6.

DISCUSSION

Consistent with most of the results reported by other authors (18–21, 26), our results suggest that cell proliferation was not affected by space conditions. We also found that levels of osteoblastic

markers, that is, alkaline phosphatase activity, P1CP, and osteocalcin, were maintained under space flight conditions. These levels were fairly constant with time and conditions (microgravity, 1 ×g in-flight and ground controls) despite increased protein content and cell number. Despite the use of buffered media, the culture conditions, mainly characterized by the absence of CO_2 exchange, accounted for the relative decrease of cellular activities during the 6 days of culture. The lack of difference in protein synthesis and P1CP, fibronectin, or alkaline phosphatase activity (18, 27, 38) in microgravity has already been reported. However, at the gene level, lower expressions for alkaline phosphatase, osteocalcin, and collagen type I mRNAs were detected in some studies (20, 28, 39), but not all (19). From these results, we can assume that despite nonstandard culture conditions, microgravity does not markedly affect cell viability and osteoblastic phenotype, suggesting that the cells used in these studies remain healthy regardless of the conditions.

Cell shape changes and cytoskeletal alterations have been reported by several investigators under microgravity conditions in both adherent and nonadherent cells (7, 16, 29, 30). Adhesion plaques that link the intracellular cytoskeleton to the extracellular matrix and trigger a myriad of intracellular signals have a recognized role in mechanotransduction both in mechanical stress models (31, for review) and in the case of gravitational stresses such as those exerted by parabolic flights (15). The present study is the first to provide quantitative data on cell adhesion after microgravity exposure. We collected two types of cell adhesion information. The first type was specifically related to integrin-mediated adhesion and was based on the detection of vinculin and phosphotyrosine at focal adhesion sites by immunostaining. The second type was not specific and represented physical contact zones at cell/substratum interface as imaged by TRIFM. The image analysis software provided 18 morphometric features describing cellular area, shape, and proportions of vinculin (and phosphotyrosine) spots as well as 6 topographic features describing the distribution of vinculin and the relative overlap of vinculin and focal contacts.

The parameters mostly affected by space exposure were related to vinculin and phosphotyrosine spots, suggesting that integrin-dependent adhesion was an effector of microgravity-related changes. The kinetics of vinculin-related changes included a decrease in the mean area of vinculin spots, followed by a more peripheral relocation of spots (Fig. 6). We can assume that these peripheral spots allowed anchorage of F-actin that effectively appeared to be exclusively cortical (Fig. 3). The mechanical environment is known to be crucial for the maintenance of cell integrity, because the cytoskeleton-generated tension forces that equilibrate external tension are mainly provided by cell-matrix and cell-cell interactions, pressures, and fluid shear stresses. This concept, called tensegrity (32), has led us to the assumption that the alteration of external forces (reduced g level, shear stress, and pressure) leads to unbalanced cytoskeletal tension at the beginning of the flight and that longer exposures will lead to a reduction of cytoskeleton-generated tensions.

Parameters derived from TIRFM (plaques) were not significantly altered by space conditions. Lack of overlap between plaques and vinculin spots (OSP) appeared early and continued to deteriorate until day 4 of flight. These results indicated that the dynamic disassembly of vinculin was not associated with parallel changes in plaque area. This was unexpected, because close contacts and focal adhesions are usually related structures formed from a common hierarchy of

molecular interactions (11, 12,). In particular, in parabolic flights, we found concomitant changes in vinculin spots and plaques (15). We therefore concluded that gravitational stresses and prolonged microgravity led to different adaptations. In microgravity, maintenance of plaques suggested an assembly of spots devoid of vinculin. Such a situation has been recently described in stretched osteoblasts, where integrin $\alpha_V\beta_3$ clusters did not colocalize with vinculin (33). Further studies are needed to fully characterize these new structures. The ability to change cellular tensegrity could modify adhesion throughout the ventral face of cells. For example, increasing cell membrane tension (or contractility) through myosin phosphorylation activated the formation of stress fibers and focal complexes assembly (34). However, when myosin phosphorylation was inhibited, integrins and vinculin dispersed from focal contacts as stress fibers and focal adhesions disassembled. In regard to these studies, our results showing disappearance of stress fibers as well as disassembly of focal complexes fit well with the assumption of a reduction in membrane contractility when cells are exposed to microgravity.

ROS 17/2.8 cell cycling appeared to occur in microgravity at a similar rate to controls, generating the same proportion of cells classified as Pre-M, M, and Post-M groups of cells. Microgravity exerted significant effects on adhesion parameters mainly in Post-M cells. In these cells, we demonstrated a relocation of vinculin spots at the cell periphery, whereas spots located between the nucleus level and cell edge disappeared. In addition, vinculin-dependent adhesion is reduced through a decreased spot number, the remaining ones being smaller. Lastly, cell spreading was reduced at this stage. However, the mean area of spots became normal during G1 to G2 transition, but this compensatory phenomenon has still to be elucidated.

In 1 g centrifuge and ground controls, homogeneous spot distribution was indicative of normal spreading and stability of cell focal adhesions. Peripheral vinculin relocation has already been described in exoenzyme C3 (inhibitor of Rho activity)-treated fibroblasts adherent to fibronectin. Such peripheral spots were considered to be precursors of focal adhesion plaques (35, 36). We can therefore speculate that focal adhesion spots generated in microgravity are less mature than those established in controls. Maturation of focal contacts is a complex process depending on the dynamics and stability of actin cables and is under the control of Rho members of GTPases (37, 38). Loss of F-actin fibers observed under flight conditions could be explained by loss of adhesion spots required for the formation of stress actin fibers. Adhesion to extracellular matrix triggers phosphorylation of a large number of signaling proteins at the focal contact, such as focal adhesion kinase, p60src, or paxillin, which, in turn, activate protein kinase C (PKC) and GTPases pathways. It has been shown that turnover of focal adhesions was found to be negatively correlated with Rho activity,and that focal adhesion kinase down-regulates Rho (39, 40). Based on the marked decrease of tyrosine phosphorylation at focal adhesion sites we observed in flight cells, we assumed that these signaling proteins could be altered in microgravity conditions

One of the most extensively studied mediators of intracellular signal transduction in eukaryotic cells is PKC. It has been shown repeatedly that gravity changes modulate PKC signaling in A431 cells (41) and various types of leukocytes (Jurkat, U937) (42–44), and there is a close correlation between PKC isoforms and the cytoskeleton, mainly actin (45) but also microtubules (46). Changes in PKC isoform distribution may therefore be associated with cellular morphologic changes. Mahler et al. (47) recently demonstrated that c-src was specifically activated by

disruption of focal contacts and that loss of adhesion was not a passive process but could activate signaling pathways that may have significant effects on cell function.

In conclusion, ROS 17/2.8 cells retained their capacity to proliferate and their osteoblastic phenotype after a 6-day microgravity exposure. Quantification of focal adhesion parameters demonstrated that microgravity acts on ROS17/2.8 cells by disorganizing cytoskeletal actin and vinculin. The kinetics of the dynamic changes affecting the area and relocation of focal contacts suggested that these structures are not only mechanoreceptors, but also mechanoeffectors. This disorganization was maximal on postmitotic cells compared with mitotic and premitotic cells and could be explained by the immaturity of the contacts established in flight. Rho-GTPase activity or downstream Rho effectors could be affected by changes in the mechanical environment experienced under microgravity conditions and might explain our results. Further experiments will be needed to precisely study GTPase activities under microgravity conditions. This experiment suggested that space-related conditions drive cytoskeletal restructuring that might control signaling cascades and thereby govern the cellular response to other stimuli such as hormones or growth factors.

ACKNOWLEDGMENTS

This work was supported by grants from the French Space Agency (CNES) n° 793/98/7134 and the European Space Agency. We wish to thank the staff of CNES, COMAT, and GSBMS for the IBIS team (especially D. Thierion, M. Viso, D. Zely, G. Gasset, and A Guell) and the staff of ESA, CCM, and Kayser Italia for the BIOBOX team (especially R. Demets, P. Baglioni, H. Willemsen, A. Koppen, G. Neri, and D Schmitt). We give special thanks to the staff of TsSKB-Progress, Russian Space Agency, for the PHOTON team (D. Kozlov and V. Abrashkine), for the use of laboratory facilities at Plessetsk, and or the technical support of our research activities.

REFERENCES

1. Hansen, L. K., Mooney D. J., Vacanti J. P., and Ingber D. E. (1994) Integrin binding and cell spreading on extracellular matrix act at different points in the cell cycle to promote hepatocyte growth. *Mol. Biol. Cell* **9,** 967–975

2. Huang, S, Chen, C. S., and Ingber, D. E. (1998) Control of cyclin D1, $p27^{Kip1}$, and cell cycle progression in human capillary endothelial cells by cell shape and cytoskeletal tension. *Mol. Biol. Cell*. **9,** 3179–3193

3. Zhu, X., and Assoian, R. K. (1995) Integrin-dependent activation of MAP kinase: a link to shape-dependent cell proliferation. *Mol. Biol. Cell*. **3,** 273–282

4. Meyer, C. J., Alenghat, F. J., Rim, P., Fong, J. H., Fabry, B., and Ingber, D. E. (2000) Mechanical control of cyclic AMP signalling and gene transcription through integrins. *Nat. Cell Biol*. **2,** 666–668

5. Frisch, S. M., Vuori, K., Ruoslahti, E., and Chan-Hui, P.Y. (1996) Control of adhesion-dependent cell survival by focal adhesion kinase. *J. Cell Biol*. **134,** 793–802

6. Dike, L. E., Chen, C. S., Mrksich, M., Tien, J., Whitesides, G. M., and Ingber, D. E. (1999) Geometric control of switching between growth, apoptosis, and differentiation during angiogenesis using micropatterned substrates. *In Vitro Cell Dev. Biol. Anim.* **35**, 441–449

7. Guignandon, A., Genty, C., Vico, L., Lafage-Proust, M. H., Palle, S., and Alexandre, C. (1997) Demonstration of feasibility of automated osteoblastic line culture in space flight. *Bone* **20,** 109–116

8. Guignandon, A., Vico, L., Alexandre, C., and Lafage-Proust, M.H. (1995) Shape changes of osteoblastic cells under gravitational variations during parabolic flight, relationship with PGE2 synthesis *Cell Struct. Funct.* **20,** 369–375

9. Wang, N., Butler, J. P. and Ingber, D. E. (1993) Mechanotransduction across the cell surface and through the cytoskeleton. *Science* **260,**1124–1127

10. Usson, Y., Guignandon, A., Laroche, N., Lafage-Proust, M. H., and Vico, L. (1997) Quantitation of cell-matrix adhesion using confocal image analysis of focal contact associated proteins and interference reflection microscopy. *Cytometry* **28,** 298–304

11. Miyamoto, S., Teramoto, H., Coso, O., Gutking, J., Burbelo, P., Akiyama, S., and Yamada, K. (1995) Integrin function: molecular hierarchies of cytoskeletal and signaling molecules. *J. Cell Biol.* **131(3),** 791–805

12. Yamada, K. M., and Geiger, B. (1997) Molecular interactions in cell adhesion complexes. *Curr. Opin. Cell Biol.* **9,** 76–85

13. Alenghat, F. J., Fabry, B., Tsai, K.Y., Goldmann, W. H., and Ingber, D. E. (2000) Analysis of cell mechanics in single vinculin-deficient cells using a magnetic tweezer. *Biochem Biophys Res Commun.* **14(277),** 93–102.

14. Schmidt, C., Pommerenke, H., Durr, F., Nebe, B., and Rychly, J. (1998) Mechanical stressing of integrin receptors induces enhanced tyrosine phosphorylation of cytoskeletally anchored proteins. *J. Biol Chem.* **273,** 5081–5085

15. Guignandon, A., Usson, Y., Laroche, N., Lafage-Proust, M. H., Sabido, O., Alexandre, C., and Vico, L. (1997) Effects of intermittent or continuous gravitational stresses on cell-matrix adhesion: Quantitative analysis of focal contacts in osteoblastic ROS 17/2.8 cells. *Exp. Cell Res.* **236,** 66–75

16. Papaseit, C., Pochon, N., and Tabony, J. (2000) Microtubule self-organization is gravity-dependent. *Proc. Natl. Acad. Sci.* **97(15),** 8364–8372

17. Tjandrawinata, R. R., Vincent, V. L., and Hughes-Fulford, M. (1997) Vibrational force alters mRNA expression in osteoblasts. *FASEB J.* **11(6),** 493–500

18. Hughes-Fulford, M., and Lewis, M. L. (1996) Effects of microgravity on osteoblast growth activation. *Exp. Cell Res.* **224,** 103–109

19. Harris, S. A., Zhang, M., Kidder, L. S., Evans, G. L., Spelsberg, T. C., and Turner, R. T. (2000) Effects of orbital spaceflight on human osteoblastic cell physiology and gene expression. *Bone* **4,** 325–331

20. Landis, W. J., Hodgens, K. J., Block, D., Toma, C. D., and Gerstenfeld, L. C. (2000) Spaceflight effects on cultured embryonic chick bone cells. *J. Bone Miner. Res.* **15,** 1099–1012

21. Kumei, Y., Shimokawa, H., Katano, H., Hara, E., Akiyama, H., Hirano, M., Mukai, C., Nagaoka, S., Whitson, P. A., and Sams, C. F. (1996) Microgravity induces prostaglandin E2 and interleukin-6 production in normal rat osteoblasts: role in bone demineralization. *Biotechnol.* **47,**
313–324

22. Guillaud, P., du Manoir, S., and Seigneurin, D. (1989) Quantification and topographical description of ki-67 antibody labelling during cell cycle of normal fibroblastic (MRC-5) and mammary tumor cell lines (MCF-7). *Anal. Cell Pathol.* **1(1),** 25–39

23. Du Manoir, S., Guillaud, P., Camus, E., Seigneurin, D., and Brugal, G. (1991) Ki-67 labeling in postmitotic cells defines different Ki-67 pathways within the 2c compartment. *Cytometry* **12(5),** 455–463

24. Lowry, O. H. (1957) Micromethods for the assay of enzymes. *Meth. Enzymol.* **4,** 366–380

25. Mainly, B. (1986) *In Multivariate Statistical Analysis. A Primer*. Chapman & Hall Ed, London pp 86–99

26. Carmeliet, G., Nys, G., and Bouillon, R. (1997) Microgravity reduces the differentiation of human osteoblastic MG-63 cells. *J. Bone Miner. Res.* **5,** 786–794

27. Hughes-Fulford, M., and Gilbertson, V. (1999) Osteoblast fibronectin mRNA, protein synthesis, and matrix are unchanged after exposure to microgravity. *FASEB J.* **13,** S121–S127

28. Carmeliet, G., Nys, G., Stockmans, I., and Bouillon, R. (1998) Gene expression related to the differentiation of osteoblastic cells is altered by microgravity. *Bone* **5,** 139S–143S

29. Lewis, M., Reynolds, J., Cubano, L., Hatton, J., Lawless, B., and Piepmeier, E. H. (1998) Spaceflight alters microtubules and increases apoptosis in human lymphocytes (Jurkat). *FASEB J.* **12,** 1007–1025

30. Moshkov, D.A., and Savel'eva, L. N. (1991) The cytoskeleton of the Mauthner neurons in the guppy after returning from an orbital flight. *Tsitologiia.* **33,** 16–22

31. Shyy, J. Y., and Chien, S. (1997) Role of integrins in cellular responses to mechanical stress and adhesion. *Curr Opin Cell Biol*. **9,** 707–13

32. Ingber, D. (1999) How cells (might) sense microgravity. *FASEB J*. **13,** S3–S15

33. Wozniak, M., Fausto, A., Carron, C. P., Meyer, D. M., and Hruska, K. A. (2000) Mechanically strained cells of the osteoblast lineage organize their extracellular matrix through unique sites of alphavbeta3-integrin expression. *J. Bone Miner. Res*. **15(9),** 1731–1745

34. Chrzanowska-Wodnicka, M. and Burridge, K. (1996) Rho-stimulated contractility drives the formation of stress fibers and focal adhesions. *J. Cell Biol*. **133,** 1403–1418

35. Clark, E., King, W., Brugge, J., Symons, M., and Hynes, R. (1998) Integrin-mediated signals regulated by members of the Rho family of GTPases. *J Cell Biol*. **18,** 3936–3946

36. Rottner, K., Hall, A., and Small, J. V. (1999) Interplay between Rac and Rho in the control of substrate contact dynamics. *Curr. Biol*. **9,** 640–648

37. Ridley, A., and Hall, A. (1992) The small GTP-binding protein Rho regulates the assembly of focal adhesions and actin stress fibers in response to growth factors. *Cell* **70,** 390–399

38. Nobes, C., and Hall, A. (1999) Rho GTPases control polarity, protrusion, and adhesion during cell movement. *J. Cell Biol*. **144,** 1235–1244

39. Xiang-Dong, R., Kiosses, W., Sieg, D., Otey, C., Schlaepfer, D., and Schwartz, M. (2000) Focal adhesion kinase suppresses Rho activity to promote focal adhesion turnover. *J. Cell Sci*. **113(20),** 3673–3678

40. Defilippi, P., Venturino, M., Gulino, D., Duperray, A., Boquet, P., Fiorentini, C., Volpe, G., Palmieri, M., Silengo, L., and Tarone, G. (1997) Dissection of pathways implicated in intergin-mediated actin cytoskeleton assembly. Involvement of protein kinase C, Rho GTPase and tyrosine phosphorylation. *J Biol. Chem*. **272,** 21726–21734

41. Rijken, P., Boonstra, J., Verkleij, A., and de Laat, S. (1994) Effects of gravity on the cellular response to epidermal growth factor. *Adv. Space Biol. Med*. **4,** 159–188

42. Schmitt, D., Hatton, J., Emond, C., Chaput, D., Paris, H., Levade, T., Cazenave, J., and Schaffar L. (1996) The distribution of protein kinase C in human leukocytes is altered in microgravity. *FASEB J*. **10,** 1627–1634

43. Limouse, M., Manie, S., Konstantinova, I., Ferrua, B., and Schaffar, L. (1991) Inhibition of phorbol ester-induced cell activation in microgravity. *Exp Cell Res*. **197,** 82–88

44. Hatton, J., Gaubert, F., Lewis, M., Darsel, Y., Ohlmann, P., Cazenave, J., and Schmitt, D. (1999) The kinetics of translocation and cellular quantity of protein kinase C in human leukocytes are modified during spaceflight. *FASEB J*. **13,** S23–S33

45. Lim, Y., Kang, S., Park, T., Lee, Y., Chun, J., and Sonn, J. (2000) Disruption of actin cytoskeleton induces chondrogenesis of mesenchymal cells by activating protein kinase C-alpha signaling. *Biochem Biophys Res Commun*. **273,** 609–622

46. Whelan, R., Kiley, S., and Parker, P. (1999) Tetradecanoyl phorbol acetate-induced microtubule reorganization is required for sustained mitogen-activated protein kinase activation and morphological differentiation of U937 cells. *Cell Growth Differ*. **10,** 271–278

47. Mahler, P. (2000) Disruption of cell-substrate adhesion activates the protein tyrosine kinase pp60c-src. *Exp. Cell Res*. **260(2),** 189–198

Received January 30, 2001; revised May 9, 2001.

Table 1

Biochemical markers of ROS17/2.8 phenotype[a]

Markers	Days	Groups			N
		Ground	Centrifuge	Flight	
					Images
Number of cells per image	0	3.68 (1.2)			30
	1	4.78 (1.3)	5.67 (1.6)	5.26 (1.5)	25
	2	6.45 (2.4)	7.62 (1.2)	6.12 (2.3)	28
	4	11.32 (3.4)	12.25 (2.7)	11.95 (3.1)	24
					Cultures
	0	150 (35)			4
Protein content (μg/well)	4	442 (81)	473 (54)	461 (75)	4
	6	458 (78)	483 (117)	495 (101)	4
					Cultures
Alkaline phosphatase	4	212 (59)	190 (n = 1)	225 (112)	3
Activity	6	260 (81)	240 (n = 1)	161 (65)	3
(nM/mg/min)					
					Cultures
Osteocalcin	0	30 (5)	32 (6)	27 (12)	6
production	2	28.5 (10)	29 (8)	30.5 (7)	6
(ng/ml)	4	28 (9)	27.5(7)	26 (8)	6
	6	25.5 (7)	24.5 (9)	24 (10)	6
					Cultures
Carboxyterminal type I collagen	0	14 (3)	15.5 (5)	15 (8.6)	6
Collagen propeptide (P1CP)	2	16 (7.2)	17 (3.4)	14.5 (6.3)	6
Production (ng/ml)	4	17 (6.2)	14 (4.6)	15 (5.3)	6
	6	16 (3.3)	12 (3.1)	17 (6.8)	6

[a]All data are presented as mean (SD). No significant difference were found between ground, centrifuge, and flight groups.

Table 2

A. Factorial discriminant analysis of cells as a function of time spent in microgravity

Stepwise factorial discriminant analysis (14 groups)		
Parameters	Step	Discriminant power
Mean area of vinculine and phosphotyrosine (PY20) spots (MS)[a]	1	91.1
Relative (/CA) area of spots (RS)[b]	2	45
Overlap of spots areas with plaques areas (OSP	3	36
Average distance of spots from cell edge (DS)	4	20
Relative (/CA) area of plaques (RP)	5	11.4
Cell area (CA)	6	10.8
Mean number of spots per cell (N)	7	9.8
Average distance of plaques from cell edge (DP)	8	7.1

[a]MS is the most dicriminant parameter in ground groups comparison (G0, G1, G2, and G4) and is the most dicriminant parameter in centrifuge groups comparison (C0, C1, C2, and C4).
[b]RS is the most dicriminant parameter in flight groups comparison (F0, F1, F2, and F4).

B. Matrix classification of cells as a function of time spent in microgravity

Matrix of classification														
Groups	BC	T0	G0	C0	F0	G1	C1	F1	G2	C2	F2	G4	C4	F4
Total correct (%)	64.9	18.1	9.4	16.4	36.7	62.2	8.2	37.8	33.3	58.7	14.4	27.4	47	62.2

Table 3

A. Factorial discriminant analysis of cells according to cell cycle phases

Stepwise discriminant analysis (Premitotic [Pre-M], mitotic [M], and postmitotic groups [Post-M]—nine groups)		
Parameters	Step	*Discriminant power*
Number of spots per cell (N)[a]	1	68.2
Mean area of spots (MS)[b]	2	44.6
Average distance of spots from cell edge (DS)[c]	3	29.3
Cell area (CA)	4	26.1
Relative (/CA) area of spots (RS)	5	8.4
Relative (/CA) area of plaques (RP)	6	6.3
Overlap of spots areas with plaques areas (OSP)	7	5.9
Average distance of plaques from cell edge (DP)	8	5.8

[a]N is the most dicriminant parameter in Post-M groups comparaison (Post-M G4, Post-M C4, Post-M F4).
[b]MS is the most dicriminant parameter in M groups comparison (M G4, M C4, M F4).
[c]DS is the most dicriminant parameter in Pre-M groups comparaison (Pre-M G4, Pre-M C4, Pre-M F4).

B. Matrix classification of cells according to cell cycle phases

Matrix of classification									
Groups	G4 Pre-M	C4 Pre-M	F4 Pre-M	G4 M	C4 M	F4 M	G4 Post-M	C4 Post-M	F4 Post-M
Total correct (%)	14.9	11.2	28.4	39.1	37.6	46.4	64.3	61.6	60.8

Table 4

Evolution of discriminant parameters as a function of cell cycle phases after a 4-day space flight conditions exposure

Discriminant parameters	N			MS (µm²)			DS (%)			CA (µm²)		
Conditions[a]	Ground	Centrif	Flight	Ground	Centri	Flight	Ground	Centri	Flight	Ground	Centri	Flight
Premitotic cells[a]	61 (19)	65 (11)	46 (8)[b]	0.72 (0.15)	0.75 (0.2)	0.74 (0.3)	34 (4)	32 (5)	25 (3)[b,c]	920 (124)	1006 (121)	676 (182)[b,c]
Mitotic cells[a]	28 (15)	24 (10)	19 (9)	1.1 (0.5)	0.71 (0.2)	0.9 (0.16)	36 (6)	34 (4)	29 (5)	340 (84)	365 (108)	334 (64)
Postmitotic cells[a]	53 (9)	52 (11)	41 (8)[b,c]	0.82 (0.22)	0.83 (0.15)	0.32 (0.2)[b,c]	34 (6)	31 (3)	21 (4)[b,c]	962 (131)	994 (153)	618 (101)[b,c]

[a]Mean (SD)
[b]$P < 0.01$ vs. centrifuge.
[c]$P < 0.01$ vs. ground.

Fig. 1

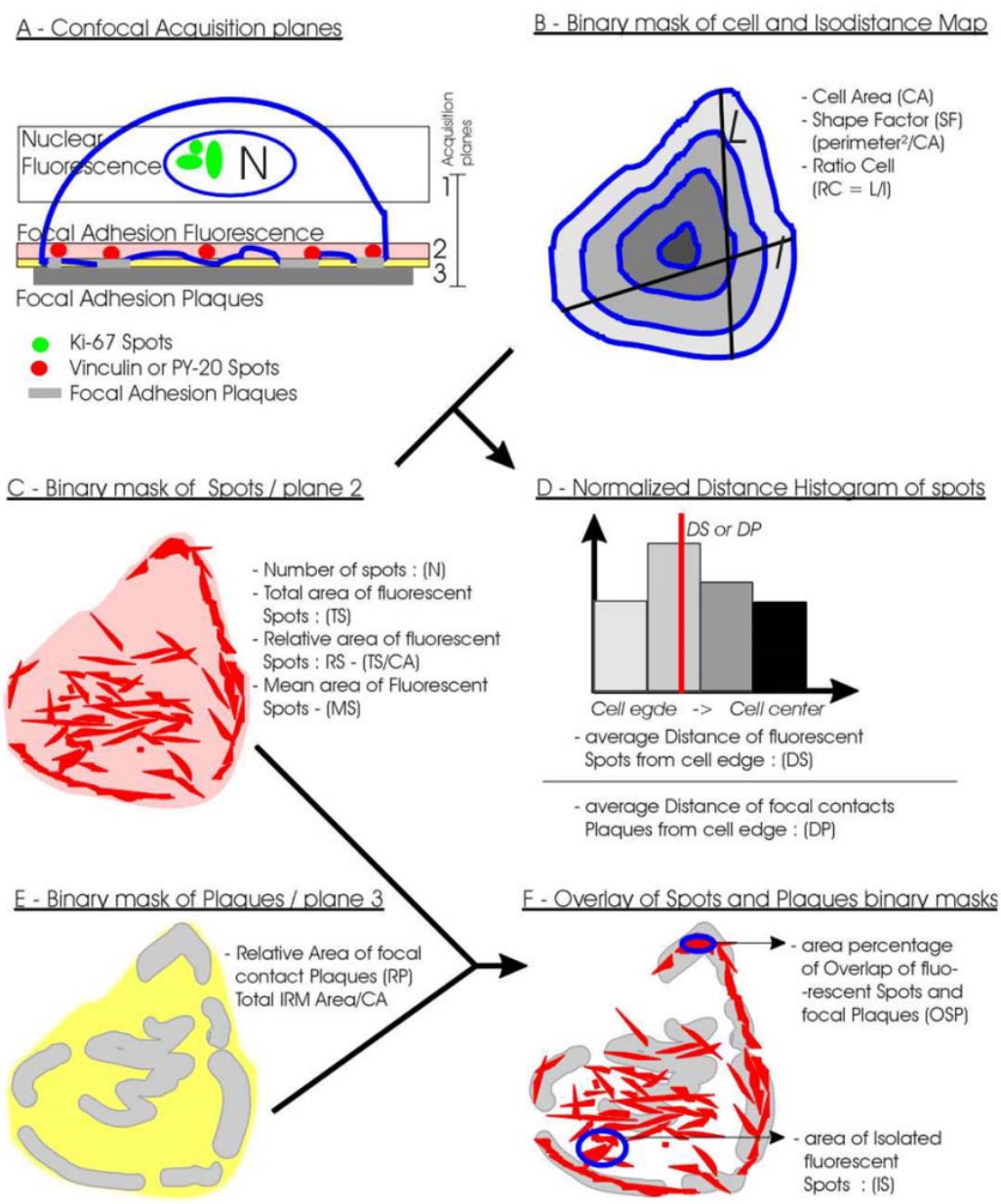

Figure 1. Diagram of the image analysis procedures from image acquisition to calculation of morphological and topographical parameters. A) Three confocal acquisition planes were used for 1) nuclear fluorescence of Ki-67, staining (green), which was collected by enhancing the pinhole (i.e., the observation plane=value of the confocal microscope to 50; 2) for restricted observation of vinculin, or PY-20 (red), which was made with a pinhole value of 20; focus set inside the cell was 0.5 μm; and 3) for nterference reflection (TIRFM) imaging. The interface between the cell membrane and the glass coverslip was found by changing the focus until the maximum reflected light was obtained. **B)** An isodistance map is calculated from the binary mask of the cell; each layer corresponds to pixels whose distance from the closest edge pixel is the same. **D)** A histogram of the distances is calculated by intersecting the distance map (B) either with the mask of vinculin or PY-20 spots **(C)** and the TIRFM binary mask of plaques **(E)**. **F)** Overlay of binary mask of spots and plaques led to calculation of overlap of contacts areas (OSP) or calculation of isolated spots of fluorescence (IS).

Fig. 2

A

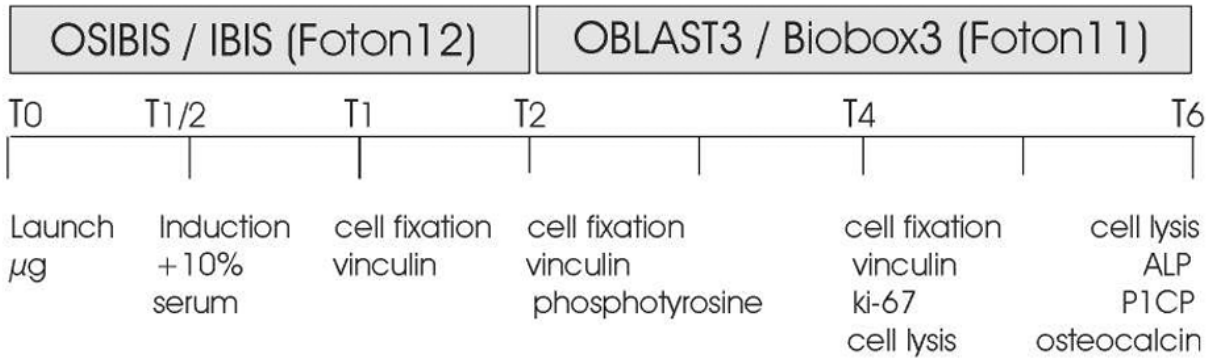

B

	BC	T0	G0	C0	F0	G1	C1	F1	G2	C2	F2	G4	C4	F4
Days of microgravity	0	0	0.5	0.5	0.5	0	1	1	0	2	2	0	4	4
Days of culture	7	3	3.5	3.5	3.5	4	4	4	5	5	5	7	7	7
g level	1	1	1	1	~0	1	1	~0	1	1	~0	1	1	~0
Serum induction	+	-	-	-	-	+	+	+	+	+	+	+	+	+

BC : Basal Control, T0 : Pre-flight Control, G : Ground, C: Centrifuge, F : Flight

Figure 2. A) Timeline of the protocol; time is indicated in days (T2 = 2 days), indicating actions performed during missions as well as postflight investigations such as vinculin staining at T1, T2, and T4 (ALP, lkaline phosphatase activity; P1CP, C-terminal type I collagen propeptide). **B)** Table summarizing the days of culture and microgravity, serum induction status, and g level experienced for all the studied groups.

Fig. 3

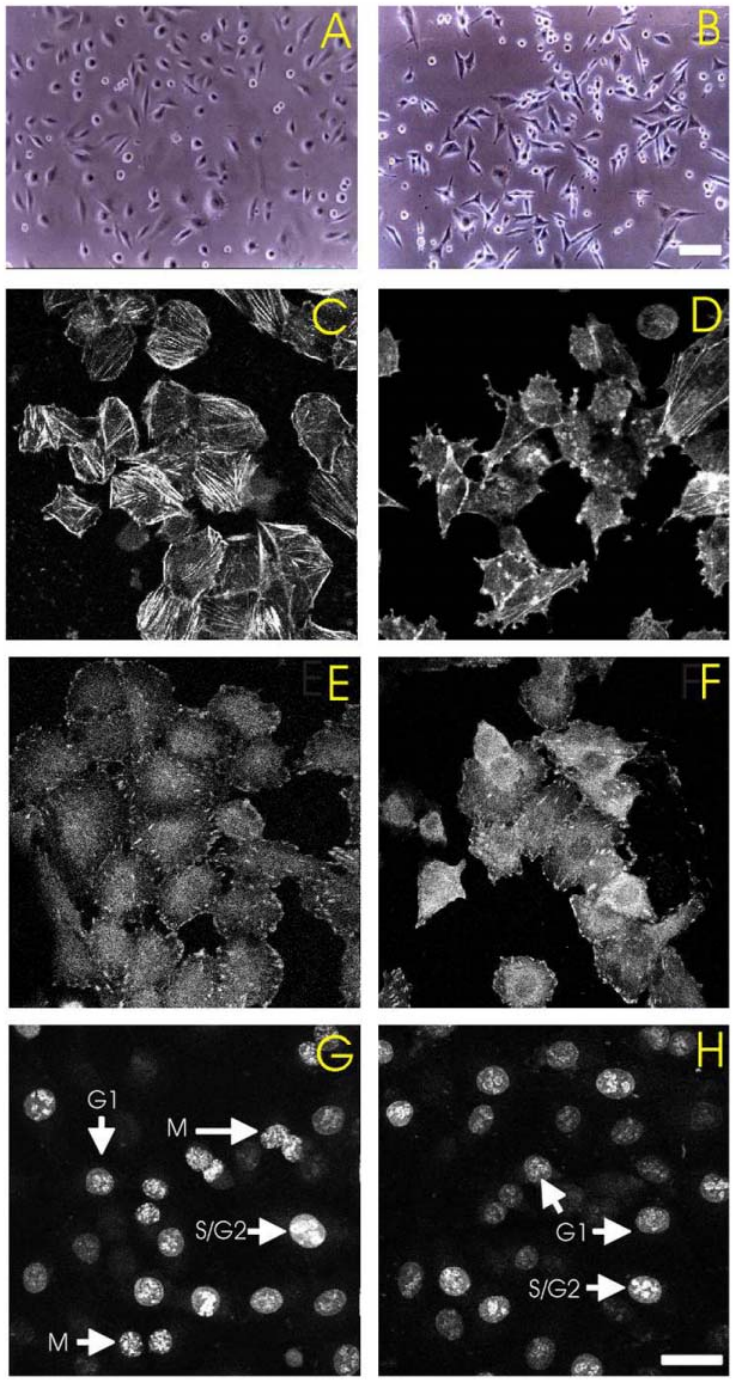

Figure 3. Observation by phase contrast microscopy of cell morphology after 4 days of culture. A) Centrifuge in-flight controls and **B)** flight culture: Note that after 4 days a large proportion of flown cells are retracted or round compared with the well-spread morphology of centrifuge. Confocal microscopy analysis of the 2-day centrifuged group of cells (C, E, and G) and microgravity-exposed cells (D, F, and H). **C)** Centrifuge controls stained for F-actin and **D)** centrifuge stained for F-actin: Note that F-actin is restricted to cell edge (filopodia-like extensions) and rarely organized in stress fibers compared with the centrifuge well-organized cytoskeleton. **E and F)** Representation of vinculin patterns indicating an important diffusion of vinculin out of focal contacts in flight cells. **G and H)** Arrows indicate G1, M, and S/G2 cell-cycle phases discriminated by Ki-67 staining topography. Note that flight cells are cycling normally. Bars: 50 μm (A and B), 15 μm (C–H).

Fig. 4

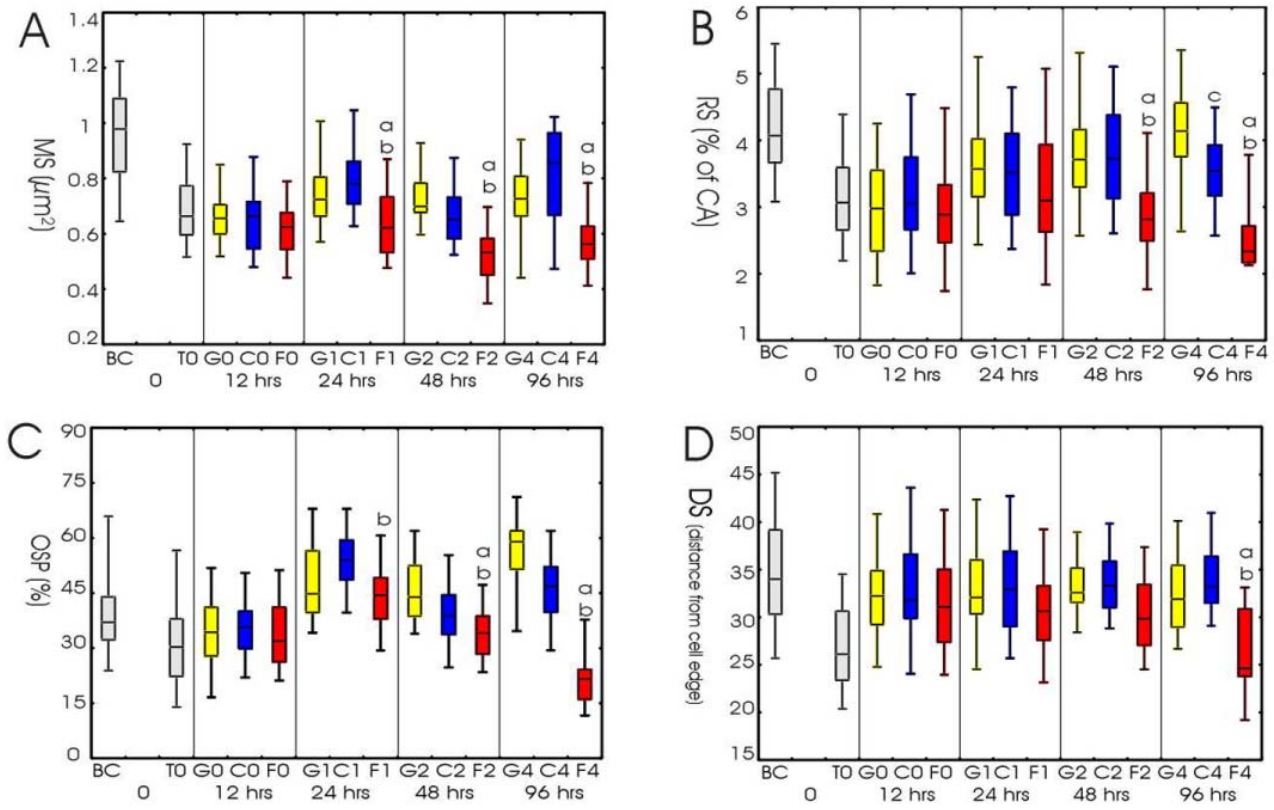

Figure 4. Box plots and whiskers of the most discriminant parameters, comparison between ground (G), centrifuge (C), and flight groups (F) (BC, basal control; T0, control without serum; and 0, 1, 2, and 4 indicating the time of culture in days. **A)** Box plots and whiskers of mean area of vinculin spots (MS): Upper and lower lines indicate the 10th and 90th percentiles, boxes indicate the 25th and 75th percentiles, and the line in the box indicates the median. Significant decrease in MS (a, b) was observed as early as 1 day in microgravity and remained reduced up to 4 days. **B)** Evolution of relative area of vinculin spots (RS). Significant decrease in this parameter was found after 2 and 4 days of microgravity, explained by a concomitant decrease in MS and in the number of adhesion spots (N; data not shown). **C)** OSP illustrates overlapping areas of vinculin spots and plaques and indicates the level of interaction between these two types of focal adhesion. The kinetics of this parameter followed the spots area one (RS), indicating that plaques were less affected or dynamic in microgravity compared with vinculin spots. **D)** Distance from cell edge (DS) is the most discriminant topographic parameter and illustrates that spots are preferentially distributed to the periphery of the cell after 4 days of flight; DS was not affected for shorter periods, indicating that redistribution of spots in microgravity is dependent of new cell generation. (a, $P<0.01$ F vs. G; b, $P<0.01$ F vs. C; c, $P<0.01$ C vs. G).

Fig. 5

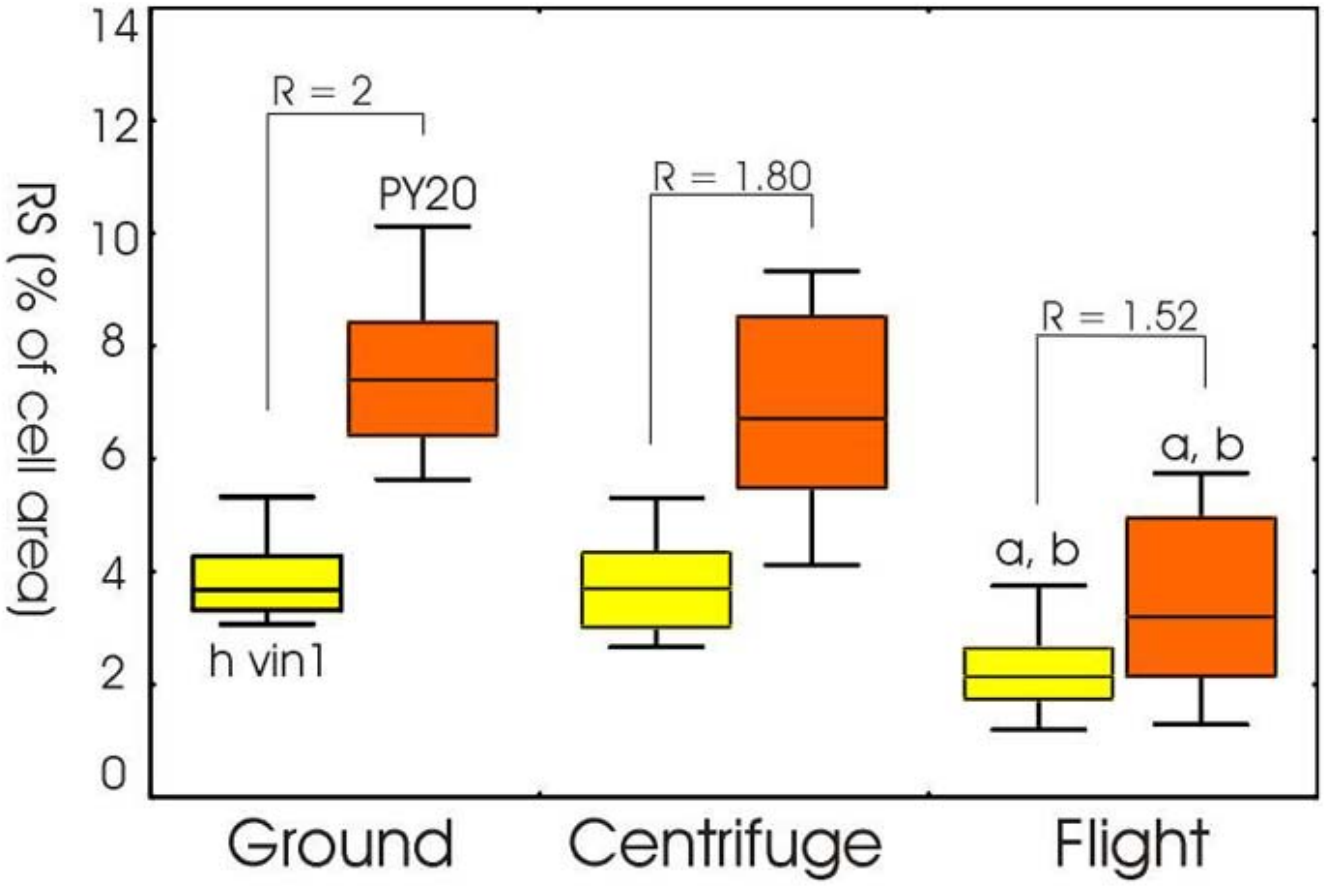

Figure 5. Comparison of relative area (RS) of vinculin spots (left named h-vin) and phosphotyrosine spots (right named PY-20) in ground, centrifuge, and flight groups after 2 days of microgravity. The vinculin and PY-20 relative areas were significantly reduced in microgravity. Note that in ground and centrifuge conditions, focal contacts contained a high proportion of tyrosine-phosphorylated proteins indicated by the ratio between mean area of PY-20 relative area/mean area of vinculin relative area (R=1.8–2) compared with the ratio obtained in flight groups (R=1.52), indicating that the potential signaling of focal contact area was reduced in microgravity as well as the focal contact area itself. (a, $P<0.01$ F vs. G; b: $P<0.01$ F vs. C; c: $P<0.01$ C vs. G).

Fig. 6

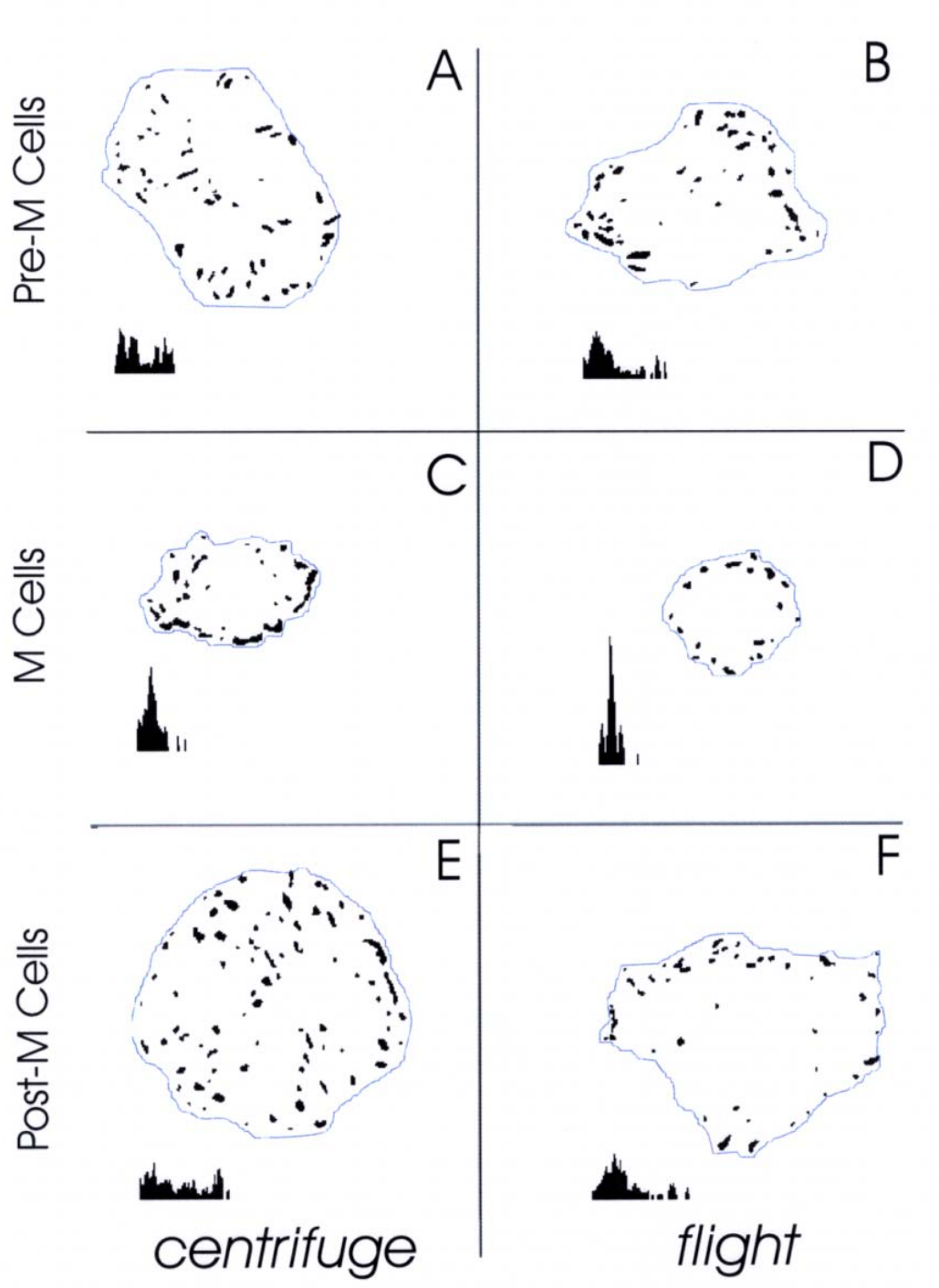

Figure 6. Representative example of binary mask of vinculin spots and normalized distance histogram were presented for each cell-cycle phase (premitotic, pre-M; mitotic, M; and postmitotic, post-M cells). Note that post-M cells in flight conditions show a smaller cell area and the absence of central spots. This illustrates that cell-cycle progression occurred in flight and suggests that spreading of post-M ROS 17/2.8 cells is modified by microgravity. It appeared that in flight conditions (right column) cells are more irregular in shape (higher shape factor indexes) presented distance histogram of spots restricted in periphery of the cell (cell edge peak) explained by disappearance of stable, central contacts leading to disorganization of ROS cytoskeleton characterized by the absence of actin stress fibers.